THE UNIVERSITY
OF ADELAIDE
AUSTRALIA

Investigation of Passive Control Devices for Potential Application to a Launch Vehicle Structure to Reduce the Interior Noise Levels During Launch

Final Report for Stage 3B

Prepared For: AFOSR
Contract Number: F62562-03-C-0029

Prepared by: Dr. Carl Q. Howard
Professor Colin H. Hansen
Mr. Rick Morgans
Dr. Anthony C. Zander
Address: School of Mechanical Engineering
The University of Adelaide
SA 5005
Australia

Contents

1 Executive Summary **3**

2 Introduction **6**
2.1 Background 6
2.2 Objectives 7

3 Unexpected Issues from Stage 3A Work **11**
3.1 Symmetric Matrices 11
3.2 Pseudo-static correction factors 14
3.3 Optimisation using genetic algorithms 15
3.3.1 Introduction 15
3.3.2 Results 16

4 Feasibility of Stage 4 Tasks **25**
4.1 Stage 4 Task 1: RSLVF optimal and sub-optimal performance evaluation 25
4.2 Stage 4 Task 2: Optimal design of multi-degree-of-freedom vibro-acoustic absorbers 26
4.3 Stage 4 Task 3. Incorporation of practical phenomenon into the modeling and design process 26
4.4 Stage 4 Task 4. Incorporation of measured data into modeling and design tools 27

5 Conclusions **30**
5.1 Summary 30
5.2 Future Work 31

A Modal Analysis of a Tube **32**

Chapter 1

Executive Summary

The work described here is directed at optimising passive vibration and acoustic devices to minimise the transmission of low frequency rocket motor noise into structures that represent launch vehicle fairings. The work was divided into three stages and this report describes the results for the second part of the third stage of the work.

In the stage 1 study, the optimal configuration of a Passive Vibro-Acoustic Device (PVAD) mounted to the interior of a small cylinder was investigated. The PVAD consisted of an acoustic absorber and a vibration absorber (Tuned Mass Damper, TMD) in the one device, and it was mounted to a flexible aluminum panel used as the cylinder end cap. A mathematical framework was developed that used modal analysis results from a finite element model together with modal coupling theory to calculate the interior acoustic pressure and structural vibration levels. The study found that the optimal PVAD design used the TMD essentially as a mass, as the uncoupled resonance frequency of the TMD was just below the upper bound of the frequency band of interest and that the optimal loudspeaker diaphragm configuration was highly lossy so that it reduced the modal amplitude of a single acoustic mode.

The objectives of the stage 2 task were to transfer the techniques developed in the stage 1 task to the optimisation of structures that more realistically represent real launch vehicles; in particular, a large composite cylinder under construction at Boeing, and a Representative Small Launch Vehicle Fairing (RSLVF). The modal coupling framework was extended to include the effects of the PVADs. A Genetic Algorithm was used to

find optimum parameters for the PVADs that would reduce a cost function, the interior acoustic potential energy in this case. It was found that the calculation of the cost function took an excessive length of time, and attempts were made at reducing the calculation time by reducing the number of modes in the analysis. Vibration and acoustic modes that did not significantly contribute to the acoustic potential energy were removed from the matrices, which decreased the calculation time. However, this action resulted in a reduction in the number of possible optimum configurations where the vibro-acoustic energy could be re-arranged into poor radiating modes and was thus considered an unsatisfactory approach for optimization of arbitrary vibro-acoustic systems.

The work listed below, that was completed in this current stage 3B, addresses some of the limitations found in stage 2 and 3A.

- The mathematics for the coupling of the passive vibro-acoustic devices to the vibro-acoustic system was re-formulated. The new framework is easily extendable to multi-degree of freedom absorbers, which enables the inclusion of torsional motion for the tuned mass dampers, and multi-resonance Helmholtz resonators. This work was anticipated to commence in stage 4.

- A distributed computing network was created using the faculty's computing pool. The use of this computing network was vital for the optimisation work that was conducted in this stage. It takes about 6 minutes to calculate the cost function on a single 3.0 GHz Pentium PC. Most of the optimisations conducted in this stage of work involved conducting 18,000 cost function evaluations. Using a single computer this would have taken about 75 days per optimisation. The use of the faculty's distributed computing network reduced the calculation time to about 3 days - 25 times faster than using a single computer.

- Several analyses were conducted to investigate the sensitivity of the interior noise reduction to parameters such as shell thickness, air temperature, acoustic damping, total mass and volume of the passive vibro-acoustic devices. The results show

that increasing the interior acoustic damping provides the greatest noise reduction compared to any method examined in this report.

- The genetic algorithm that was used for the optimisation in stage 2 used an integer representation for the chromosomes. The conclusion from the work was that an integer representation limited the evolution process, and that a binary string representation should be used. In stage 3A, a binary string representation was used, which did not appear to stunt the evolution process. However it was found in the current work that the integer representation gives just as good results in half the time, so this method was retained for the current work. The genetic algorithms developed in this stage were modified for use with the distributed computing network.

- Not all of the modal coupling formulation work was completed as planned in the current stage. However, some of the work planned for stage 4 was completed instead as explained in the report. Thus, the remainder of the work to complete the modal coupling formulation will be completed as part of the stage 4 work.

Chapter 2

Introduction

2.1 Background

The worked discussed in the following report was undertaken as a follow on of stages 1, 2, and 3A of the project that originated as a result of the work done by Dr. Steve Griffin of the Air Force Research Lab at Kirtland AFB, New Mexico during his participation in the AFOSR Windows on Science program at the University of Adelaide, South Australia in 1998. Dr. Griffin's work was a collaborative effort with the Active Noise and Vibration Control Group at the University of Adelaide and it involved an investigation of the application of active feedback control of launch vehicle structural vibration using radiation mode vibration levels as the cost function to minimise interior noise levels. The work led to the publication of three papers. That work found only a small benefit of active control, compared to the passive effect of the un-excited actuators attached to the structure. This has been the impetus behind the work conducted here, which is directed at optimising the passive effect of vibration reducing devices. The current work was divided into three stages and this report is primarily intended to provide the results for the second part of the third stage of the work.

2.2 Objectives

The following list contains the work plan of for Stage 3B (from 1 September 2003) shown in *italics*, and following each task is a bulleted list describing the work that was done.

1. Address any unexpected issues raised in the Stage 3A work

In the proposal for task 3A it was stated that if necessary and if time permitted, a re-evaluation of the modal coupling technique would be undertaken. It has since become clear that this work is necessary and that all of the time allocated to Stage 3A will be taken up with the other tasks outlined in that work statement and the re-evaluation of the modal coupling technique will need to be part of stage 3B. A possible approach to this task may be to rewrite the modal coupling code to perform a coupled eigenvalue analysis, giving the coupled natural frequencies.

The tasks that will be undertaken are:

- *investigate the implementation of a symmetric matrix formulation for the modal coupling method. Symmetric matrices are faster to invert that non-symmetric matrices, and hence the response of the vibro-acoustic system will be evaluated faster than currently.*
- *investigate the implementation of pseudo-static correction factors to account for modes outside the analysis frequency range.*
- *compare the integer and binary representations of the chromosomes and determine which method converges to the optimum solution the fastest.*

(Estimated duration: 1 month).

Work completed:

- Work was done to investigate symmetric matrix formulations for modal coupling. It was found that there is decrease in the calculation time using this formulation,

compared to the current formulation. Further work is required to extend this to the fully coupled models incorporating Helmholtz resonators and Tuned Mass Dampers.

- Investigations were conducted with pseudo-static correction factors for structural models. The mathematical framework required knowledge of the full mass and stiffness matrices in order to calculate the correction factor. While it is possible do do this for the current method, this is unlikely to yield significant benefits in terms of reducing the time for calculations.

- The asynchronous parallel genetic algorithm developed in Stage 3A was reformulated to use integer representations for the chromosomes. The results showed that the optimisations acheived the same reductions in acoustic potential energy with half the number of cost function evaluations compared to using a binary representation for the chromosomes. Thus the integer representation will be retained for all future work.

The details of the work summarised by the dot points above are discussed in chapter 3 of this report.

2. Investigate the Feasibility of Stage 4 Tasks

Preliminary work will be undertaken on Stage 4 tasks 2, 3 and 4 with a view to confirming the feasibility of the proposed approach and investigating the possibility of using alternative approaches to the absorber design and evaluation tasks, which may be preferable to the approach proposed initially. (estimated duration: 1.5 months)

Work completed:

- The Stage 4 tasks 2, 3 and 4 are listed in the conclusion chapter in the Stage 3A report. However, for clarity they are repeated below:

Task 2. Optimal design of multi-degree of freedom vibro-acoustic absorbers

- Portions of this work were completed in Stage 3A. The mathematical framework has been established.

Task 3. Incorporation of Practical Phenomena into the Modeling and Design Process

- Structural, acoustic, and boundary condition anomalies can be incorporated into the structural or acoustic finite element models and the appropriate mode shapes can be calculated and used in the modal coupling software.
- The effect of a rigid payload can be easily incorporated into the acoustic finite element model by removing some interior fluid elements. A resonant payload can be simulated as another structure within the cavity.

Task 4. Incorporation of Measured Data into Modeling and Design Tools

- The success of this task is ultimately dependent on the supply of good quality modal data and documentation of the testing procedures. Whilst this is an excellent task, the practical implementation might be difficult. It is hoped that the modal data could be used to update the finite element model mass and stiffness matrices, thereby updating the modal results and use these actual measured data in the optimisation process.
- If this task is too difficult to implement from an administrative standpoint, a suitable alternative is to replace this task with a task aimed at examining the sensitivity of the acoustic potential energy in the payload bay for several acoustic loading conditions.

Details of the work summarised above are included in chapter 4 of this report.

3. Report for Stage 3B

(estimated duration: 0.5 month)

Work completed:

- This document describes the work that was completed for Stage 3B.

Total time for Stage 3B: 3 months

Chapter 3

Unexpected Issues from Stage 3A Work

3.1 Symmetric Matrices

Many researchers have investigated the use of modal coupling methods for vibro-acoustic problems because the time to solve the equations is less than the time taken to solve the fully coupled fluid-structure interaction equations.

The modal coupling theory that was developed in Stage 1 [2] and used in Stages 2 [3] and Stage 3A [4] was based on Cazzolato's PhD thesis [5]. The equations used in the thesis were similar to those presented in Fahy's book [6].

Bokil and Shirahatti [7] have described a modal coupling method that is similar to that presented in Fahy [6], using a velocity potential formulation. Bokil and Shirahatti show how to include the rigid cavity mode in the matrix equations, thereby preventing a singularity condition in the matrices (caused by the rigid cavity mode that has a resonance frequency of 0Hz) when they are inverted to solve for the forced response. They also show a method to calculate the mode shapes and resonance frequencies for the coupled system that results in matrices that are symmetric and skew-symmetric, which are twice the dimensions of the total number of included structural and acoustic modes. Unfortunately, this method suffers from the inability to include damping in the matrices, which would

change the matrices from skew-symmetric to a general case, which counteracts the benefit of short calculation time.

Note that care should be taken in attempting to use the equations described in Bokil and Shirahatti [7], as the equations for the example of the coupled rectangular enclosure with a thin plate are incorrect, and the equations are not set out correctly for matrix multiplication and transpose operations.

Tournour and Atalla [8] have described a modal coupling formulation based on the work of Morand and Ohayon [9] and Atalla and Bernhard [10]. Unfortunately the previous work that is cited does not clarity their formulation. Their paper describes the equations governing the structural-acoustic system as

$$\begin{bmatrix} \mathbf{K} - \omega^2 \mathbf{M} & \mathbf{C} \\ \mathbf{C}^{\mathrm{T}} & \frac{1}{\omega^2}\mathbf{H} - \mathbf{Q} \end{bmatrix} \begin{bmatrix} \mathbf{u} \\ \mathbf{p} \end{bmatrix} = \begin{bmatrix} \mathbf{F} \\ \frac{1}{\omega^2}\mathbf{S} \end{bmatrix} \tag{3.1}$$

where $\mathbf{K}$ and $\mathbf{M}$ are the structural stiffness and mass matrices respectively, $\mathbf{H}$ and $\mathbf{Q}$ are the cavity kinetic energy and compressibility matrix, respectively, and $\mathbf{C}$ is the coupling matrix. Vectors $\mathbf{u}$, $\mathbf{p}$, $\mathbf{F}$, and $\mathbf{S}$ are the structural displacement, cavity pressure, force applied to the structure, and the acoustical source, respectively. One would normally expect the cavity kinetic energy to be proportional to the mass of the acoustic fluid, and the compressibility matrix proportional to the stiffness of the acoustic fluid. However, it can be seen that by multiplying the terms on the bottom row of the matrix by ω^2 would result in the terms $\mathbf{H} - \omega^2\mathbf{Q}$, where the stiffness is multiplied by the square of the frequency, which differs from the usual formulation of $\mathbf{K} - \omega^2\mathbf{M}$.

Conversion of Eqs. (6.27) and (6.28) in Fahy [6, p250] into matrix form results in the following system equations of motion

$$\begin{bmatrix} \mathbf{\Lambda}_p \left([\boldsymbol{\omega}_p]^2 - \omega^2 \right) & -S\left[\mathbf{C}_{np}\right] \\ -S\left[\mathbf{C}_{np}\right]^{\mathrm{T}} & \frac{\mathbf{\Lambda}_n}{\rho_0 c^2 \omega^2} \left([\boldsymbol{\omega}_n]^2 - \omega^2 \right) \end{bmatrix} \begin{bmatrix} \mathbf{w}_p \\ \mathbf{p}_n \end{bmatrix} = \begin{bmatrix} \mathbf{F}_p \\ \dot{\mathbf{Q}}_n / \omega^2 \end{bmatrix} \tag{3.2}$$

where $\mathbf{w}_p$, $\mathbf{\Lambda}_p$, $[\boldsymbol{\omega}_p]$, and $\mathbf{F}_p$ are the structural displacement modal participation factor, diagonal matrix of the structural modal mass, diagonal matrix of the structural resonance frequencies, and generalised modal force applied to the structure, respectively. $\mathbf{p}_n$, $\mathbf{\Lambda}_n$, $[\boldsymbol{\omega}_n]$, ρ_0, c, $\dot{\mathbf{Q}}_n$ are the modal participation factors for the acoustic pressure, diagonal matrix of the acoustic modal volume, diagonal matrix of the acoustic resonance frequencies, density of the fluid, speed of sound in the fluid, and the time derivative of the generalised acoustic source strength, respectively. $\mathbf{C}_{np}$ and S are the dimensionless coupling coefficient between the acoustic mode shape function and the structural mode shape function, and the surface area, respectively. Multiplication of the bottom elements in the matrices of Eq. (3.2) by $\rho_0 c^2 \omega^2$ results in the (2,2) term as $\mathbf{\Lambda}_n([\boldsymbol{\omega}_n]^2 - \omega^2)$, where one can see that the first term $\mathbf{\Lambda}_n[\boldsymbol{\omega}_n]^2$ is equivalent to the modal stiffness, and the second term $-\omega^2\mathbf{\Lambda}_n$ is the square of the frequency times the acoustic modal mass, which is similar in form to the typical $\mathbf{K} - \omega^2\mathbf{M}$. Hence, the (2,2) element of the matrices in Eqs (3.1) and (3.2) shows that the functional form of the two formulations is quite different.

Morand and Ohayon [9, p151] show a matrix formulation that is similar to Eq. (3.1), yet do not elucidate why their formulation differs from numerous other researchers that use Fahy's methods (for example Refs [11–15]).

Currently, the equations for the modal coupling theory used in the Matlab software are more complicated that those presented in Refs [6, 7]. The Matlab software was re-coded for the plain vibro-acoustic case without the effects of the PVADs and it was found that the time taken for a typical calculation reduced from 180s to 130s. When the damping in the system was removed, the matrices become real and the calculation time further decreased to about 30s, which is 5× faster than the calculation when damping was included. This is an encouraging outcome, because if the calculations can somehow be conducted by omitting damping to calculate the coupled mode shapes, it might be possible to include the effects of damping afterwards and still achieve a significant improvement in calculation time. Hysteretic damping models are currently used in the modal coupling theory, which have the characteristic that the damped mode shapes are not the same as the undamped

mode shapes. If the damping model was changed to proportional damping, then the damped mode shapes are the same as undamped mode shapes, only the amplitude of the modal participation factors will change.

Based on the success of the reformulating the equations from Stage 3A into a symmetric matrices using Fahy [6], additional work will be done in Stage 4 to incorporate the effect of the PVADs with a symmetric matrix formulation.

3.2 Pseudo-static correction factors

Atalla and Bernhard [10] present a symmetric matrix formulation and a pseudo-static correction factor to account for higher order modes that improves the accuracy of predictions. However, for reasons cited above the methods described in this paper were not used.

Zhao et al. [16] show a method to calculate pseudo-static correction factors for the truncated modes, that uses the full mass and stiffness matrices to calculate the correction matrices. For the problem at hand, it would be possible to extract these data from the ANSYS models; however this would involve a substantial effort in software programming that is beyond the scope of work in this stage. The results from their examples show that there is slight improvement in the accuracy at frequencies close to the end of the analysis frequency range. Their results indicate that there is little benefit in obtaining greater accuracy from reformulating the modal models, as substantial work would be necessary and hence this method will not be used.

3.3 Optimisation using genetic algorithms

3.3.1 Introduction

The work in Stage 3A used a binary representation for the chromosomes as suggested from the conclusions of Stage 2. It was subsequently suggested that comparisons should be made of the possible benefits of both binary and integer methods.

Hansen et al. [17] describe the use of an integer formulation of a genetic algorithm to optimise the location of control actuators for active-structural-acoustic-control (ASAC) (see also Refs [18, 19]). Their conclusion was that an integer representation for the location of the actuators provides faster convergence than a binary string representation. With a binary representation of the chromosomes, the cross-over process swaps bits (as in a 1 or 0) of the string between children, which can causes a large change in the location of the actuators, thereby destroying any information gained in the population from the evolutionary process. Whereas for an integer representation of the chromosomes, the cross-over process swaps the entire integer string between children and hence retains the position information in the population. The mutation of the chromosome string (which means selecting a random number to replace the existing number) is the process responsible for ensuring the process does not get stuck in a local optimum, thus failing to find the global optimum.

The results presented here show, as expected, that the convergence rate is twice as fast when using the integer string representation compared to using the binary string representation. The optimum noise reductions achieved are also similar with the two methods, indicating that the integer representation with mutation is effective in finding the global optimum.

3.3.2 Results

Figure 3.2 shows the location of 10 PVADs after 18,000 cost function evaluations (two cost function evaluations per generation) on an angular plot, where the 0° is along the X-axis, pointing towards the sound source.

Table 3.2 lists the approximate resonance frequencies of the 10 PVADs, based on the stiffness values in Table 3.1, and that the mass of the TMD and HR are 0.45kg and 0.01kg, respectively.

	Location			TMD		HR	
PVAD No.	Node	θ (degrees)	Z (m)	Stiffness ($\times 10^6$ N/m)	Damping (%)	Stiffness ($\times 10^4$ N/m)	Damping (%)
1	3378	3.2	2.24	7.11	3	1.05	18
2	5676	38.6	1.60	1.15	23	2.55	15
3	27264	-73.9	0.80	1.32	20	2.51	1
4	31517	-135.0	2.00	5.18	23	9.88	1
5	7839	61.1	1.04	6.84	23	2.88	6
6	25235	-64.3	1.20	8.95	23	1.91	6
7	9942	77.1	1.12	9.98	20	2.59	6
8	9888	70.7	2.24	9.82	11	2.47	1
9	27411	-86.8	1.68	1.93	20	2.86	3
10	27307	-77.1	1.52	8.59	15	3.56	3

Table 3.1: Value of parameters for the 10 PVADs after 18,000 cost function evaluations

PVAD No.	TMD Freq (Hz)	HR Freq (Hz)
1	424	163
2	171	254
3	183	252
4	362	500
5	416	270
6	476	220
7	503	256
8	499	250
9	221	269
10	466	300

Table 3.2: Approximate resonance frequencies of the 10 PVADs after 18,000 cost function evaluations

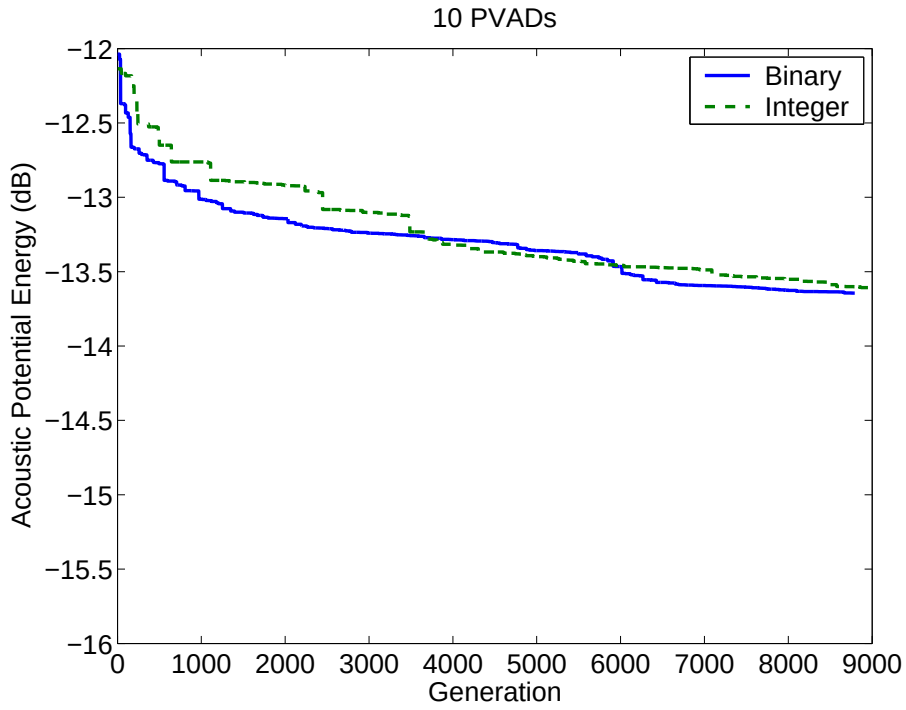

FIG. 3.1: Evolution of the genetic algorithm's cost function over 18,000 evaluations.

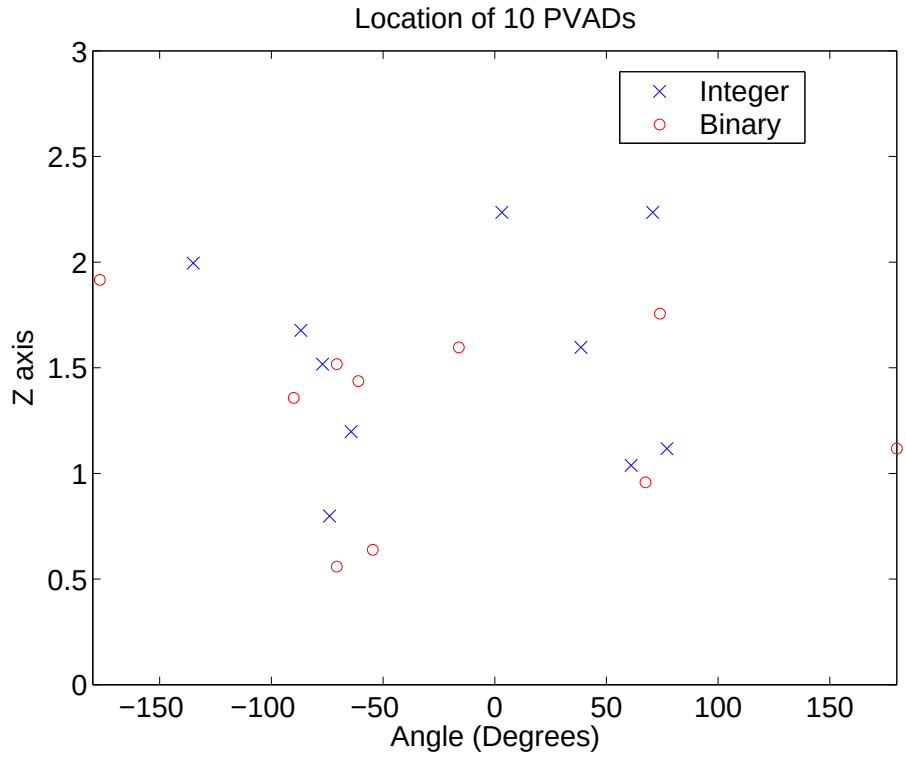

FIG. 3.2: Location of the 10 PVADs after optimisation for 18,000 cost function evaluations, as if the surface of the cylinder had been unwrapped.

Figure 3.4 shows the location of 20 PVADs after 18,000 cost function evaluations (two cost function evaluations per generation) on an angular plot, where the 0° is along the X-axis, pointing towards the sound source.

Table 3.4 lists the approximate resonance frequencies of the 20 PVADs, based on the stiffness values in Table 3.3, and that the mass of the TMD and HR are 0.45kg and 0.01kg, respectively.

	Location			TMD		HR	
PVAD No.	Node	θ (degrees)	Z (m)	Stiffness ($\times 10^6$ N/m)	Damping (%)	Stiffness ($\times 10^4$ N/m)	Damping (%)
1	3477	12.9	2.00	7.31	23	1.61	8
2	33822	-125.4	1.92	0.76	23	5.55	3
3	29540	-163.9	1.12	1.01	18	4.71	13
4	27375	-83.6	1.52	1.93	23	2.65	3
5	27305	-77.1	1.36	1.93	18	3.47	1
6	20817	-12.9	0.40	0.87	23	2.80	6
7	7801	57.9	0.72	6.90	20	2.06	8
8	22885	-25.7	0.40	2.76	23	2.61	18
9	7842	61.1	1.28	9.84	23	3.10	11
10	9813	90.0	1.68	10.00	23	2.86	8
11	33682	-112.5	1.60	2.88	23	3.37	3
12	14912	141.4	1.28	0.72	23	3.58	1
13	25007	-67.5	2.00	6.98	23	3.47	3
14	17084	118.9	1.44	6.14	18	2.45	11
15	35472	-99.6	2.39	2.04	23	2.06	18
16	7763	54.6	0.40	8.28	13	2.82	8
17	20911	-19.3	2.47	9.37	3	0.87	3
18	25227	-64.3	0.56	4.11	23	2.84	8
19	25238	-64.3	1.44	3.49	23	2.16	3
20	9945	77.1	1.36	6.86	23	3.04	11

Table 3.3: Value of parameters for the 20 PVADs after 18,000 cost function evaluations

PVAD No.	TMD Freq (Hz)	HR Freq (Hz)
1	430	202
2	139	375
3	160	345
4	221	259
5	221	297
6	148	266
7	418	228
8	264	257
9	499	280
10	503	269
11	270	292
12	135	301
13	421	297
14	394	249
15	227	228
16	458	267
17	487	148
18	323	268
19	298	234
20	417	278

Table 3.4: Approximate resonance frequencies of the 20 PVADs after 18,000 cost function evaluations

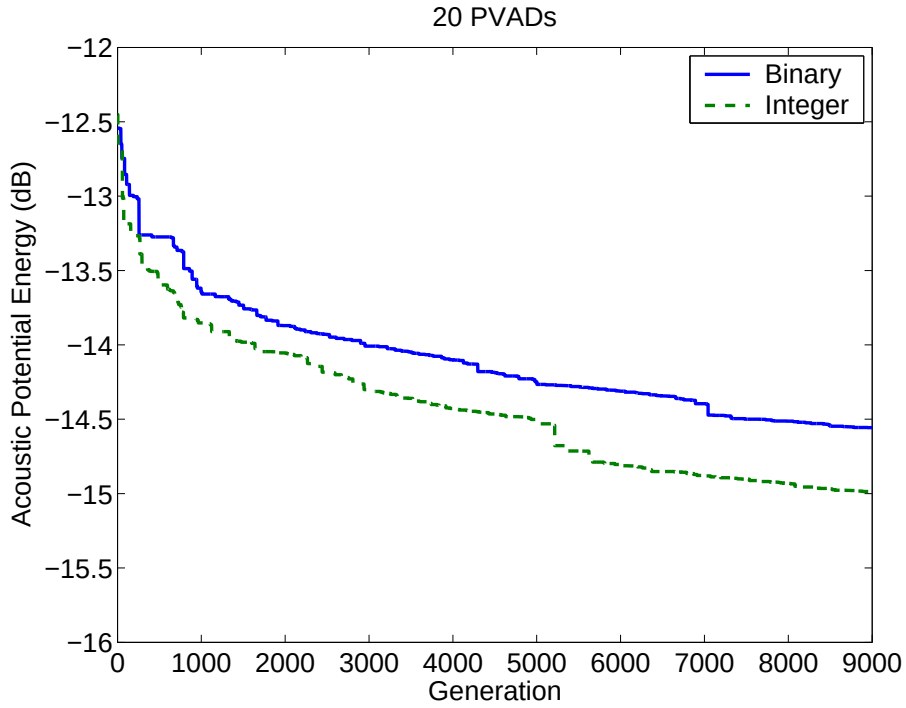

FIG. 3.3: Evolution of the genetic algorithm's cost function over 18,000 evaluations.

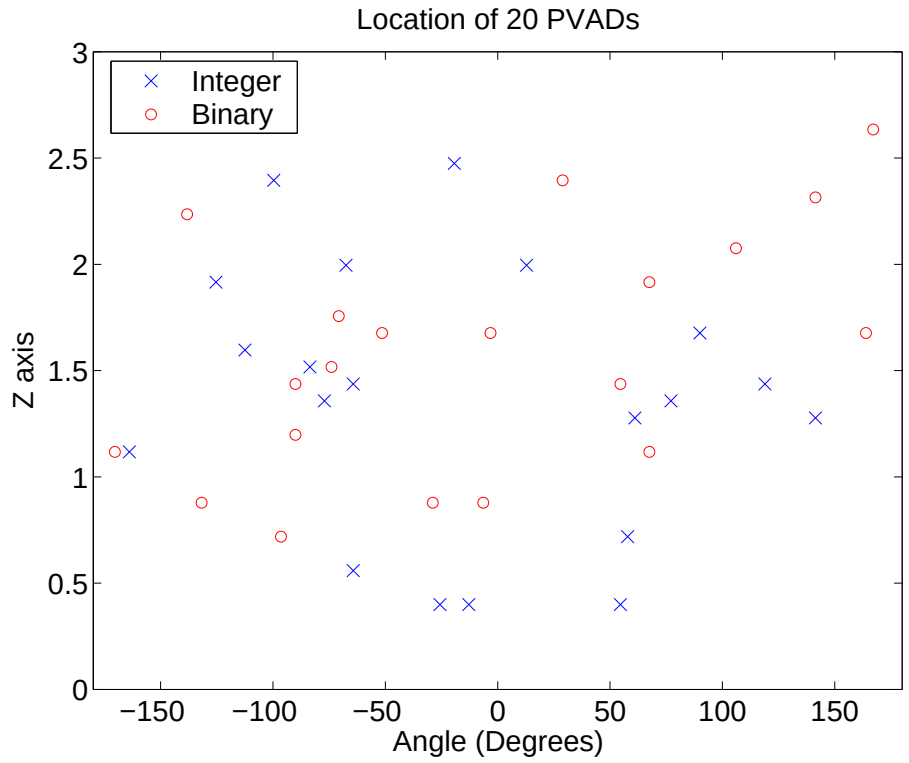

FIG. 3.4: Location of the 20 PVADs after optimisation for 18,000 cost function evaluations, as if the surface of the cylinder had been unwrapped.

Figure 3.6 shows the location of 30 PVADs after 18,000 cost function evaluations (two cost function evaluations per generation) on an angular plot, where the 0° is along the X-axis, pointing towards the sound source.

Table 3.6 lists the approximate resonance frequencies of the 30 PVADs, based on the stiffness values in Table 3.5, and that the mass of the TMD and HR are 0.45kg and 0.01kg, respectively.

	Location			TMD		HR	
PVAD No.	Node	θ (degrees)	Z (m)	Stiffness ($\times 10^6$ N/m)	Damping (%)	Stiffness ($\times 10^4$ N/m)	Damping (%)
1	27268	-73.9	1.12	1.63	23	3.27	1
2	5610	32.1	1.76	2.39	23	6.41	3
3	20862	-16.1	1.28	6.20	1	7.05	1
4	3260	22.5	0.96	0.48	18	3.51	3
5	5534	25.7	1.12	5.73	23	8.24	15
6	10049	86.8	1.52	2.26	20	1.56	15
7	17002	125.4	0.32	2.45	20	0.44	1
8	20802	-9.6	1.92	8.30	1	4.81	23
9	35427	-102.9	1.52	8.11	23	9.96	23
10	9877	70.7	1.36	3.49	20	2.86	23
11	20757	-6.4	1.04	8.42	23	6.22	1
12	7643	67.5	1.68	4.83	6	1.34	13
13	27393	-86.8	0.24	0.44	11	8.09	8
14	27243	-70.7	1.84	1.71	20	4.40	18
15	22952	-32.1	0.32	5.34	20	3.43	18
16	22904	-25.7	1.92	1.89	8	7.62	18
17	25233	-64.3	1.04	9.82	20	1.85	23
18	9998	83.6	0.16	8.67	23	1.93	6
19	7890	64.3	2.39	3.15	20	2.08	20
20	7763	54.6	0.40	1.56	18	0.07	3
21	23043	-38.6	2.16	2.76	15	9.69	13
22	22965	-32.1	1.36	8.93	18	3.41	8
23	18696	96.4	1.60	1.67	15	10.04	11
24	20748	-6.4	0.32	3.08	20	8.30	20
25	31682	-144.6	1.60	0.93	23	7.11	11
26	12505	180.0	1.36	1.48	23	5.71	8
27	25236	-64.3	1.28	5.30	15	0.74	3
28	3433	9.6	1.20	9.39	23	0.21	11
29	31723	-141.4	2.16	5.40	23	3.97	15
30	29587	-160.7	2.16	0.60	23	5.73	8

Table 3.5: Value of parameters for the 30 PVADs after 18,000 cost function evaluations

PVAD No.	TMD Freq (Hz)	HR Freq (Hz)
1	203	288
2	246	403
3	396	422
4	110	298
5	381	457
6	239	199
7	249	105
8	458	349
9	453	502
10	298	269
11	462	397
12	350	184
13	105	453
14	208	334
15	368	295
16	219	439
17	499	217
18	469	221
19	282	229
20	199	41
21	264	496
22	476	294
23	206	504
24	279	458
25	153	424
26	194	380
27	366	137
28	488	73
29	370	317
30	123	381

Table 3.6: Approximate resonance frequencies of the 30 PVADs after 18,000 cost function evaluations

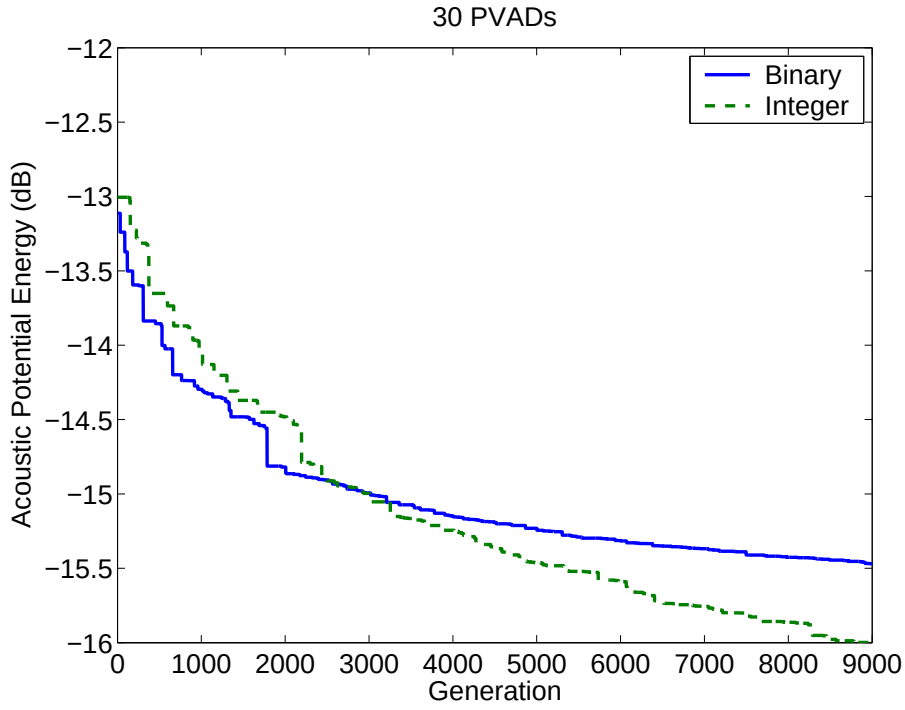

FIG. 3.5: Evolution of the genetic algorithm's cost function over 18,000 evaluations.

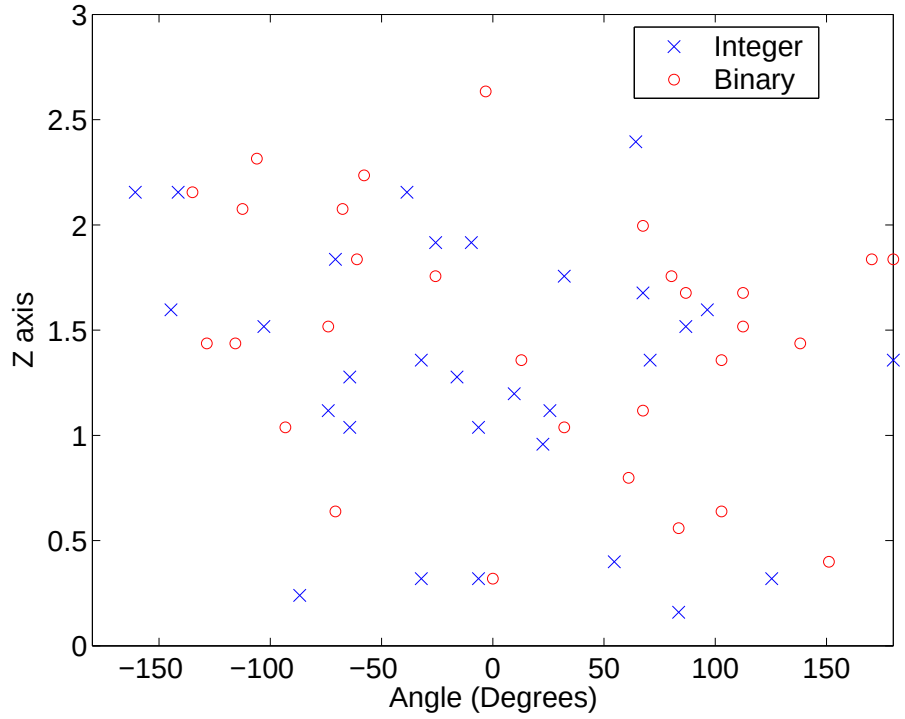

FIG. 3.6: Location of the 30 PVADs after optimisation for 18,000 cost function evaluations, as if the surface of the cylinder had been unwrapped.

The results in Figures 3.3 and 3.5 show that the use of the integer representation for the chromosomes evolves about twice as fast compared to using the binary representation for the chromosomes. The other interesting result is that the distribution of the PVADs is different between the use of the integer and binary representations. Some researchers have an undocumented hypothesis that for low numbers of PVADs (about 5) then the optimum location of the absorbers is fixed. However as the number of PVADs increases (about 20), then the locations of the absorbers are not critical and there are many 'optimal' locations that are scattered over the structure.

Chapter 4

Feasibility of Stage 4 Tasks

The work plan of the current stage 3B included an investigation of the feasibility of the Stage 4 tasks. The following list contains the work plan of for Stage 4 (from 1 September 2003) shown in *italics*, and following each task is a description of the feasibility of the task.

4.1 Stage 4 Task 1: RSLVF optimal and sub-optimal performance evaluation

The design tools developed in stage 3 will be applied the RSLVF fairing model. The reduction of interior noise levels shall be investigated for different design approaches for the RSLVF. Performance of the tools shall be assessed. The investigation shall include the performance of VADs, which represent vibration and acoustic absorbers at the same location, the possible benefit of separating them shall be investigated.

Mathematical tools have been developed in the project that can be used to determine optimum parameters for the locations, stiffness, mass and damping of Helmholtz resonators and Tuned Mass dampers attached to the circumference of a rocket fairing. The finite element models that were used in stage 2 and 3A were for the Boeing cylinder that was made from a composite material. The same mathematical tools can be used to analyse the Representative Scale Launch Vehicle Fairing (RSLVF). A Nastran finite

element model has been supplied by Boeing SVS, which can be re-interpreted into the ANSYS finite element software package and the modal analyses conducted to extract the in-vacuo mode shapes and resonance frequencies for the structure and acoustic cavity. These mode shapes and resonance frequencies can be used by the Matlab modal coupling software, without any software modifications.

4.2 Stage 4 Task 2: Optimal design of multi-degree-of-freedom vibro-acoustic absorbers

The design of a multi-degree-of-freedom vibro-acoustic absorber with rocking modes and a twisting mode in addition to the normal translational modes will be investigated. Key design issues shall be identified and design techniques developed.

The mathematical framework developed in Stage 2 was not amenable to extension to multi-degree of freedom absorbers. Hence, part of the Stage 3A work included reformulating the modal coupling method to incorporate the Helmholtz resonators and Tuned Mass Dampers that could be extended to multi-degree of freedom systems. This was done by adapting the framework presented in Refs [1, 20]. Hence part of the work that was due only to start in Stage 4 has already been completed.

4.3 Stage 4 Task 3. Incorporation of practical phenomenon into the modeling and design process

Having developed efficient computation methods in task 4.1, and having developed improved PVAD devices in task 4.2, the effects of the following practical phenomena will be investigated:

- *structural anomalies including a vent, a separation seam, and/or a variation in the boundary conditions, and*

- *Acoustic fill including the determination of the effect of having a rigid payload and a resonant payload in the interior volume.*

Structural anomalies, such as stiffening rings, variations in the thickness of the fairing, lumped masses on the fairing, various boundary conditions, etc., can all be accounted for in the vibro-acoustic models, by appropriately creating representative structural finite element models. However, care has to be taken when extracting the structural modal analysis results that only the nodes and elements that are in contact with the acoustic fluid are included in the output files.

Similarly, the modelling of various interior acoustic conditions can be accomplished by creating the appropriate finite element model of the acoustic fluid. If the interior has a rigid payload, such as a cube, then the fluid elements are removed from the location of the rigid box, to simulate a rigid walled object.

The effect of a vent can be modelled by two methods. One method involves defining the nodes on the circumference of the cylinder with a pressure boundary condition of zero Pascals. This has the effect of simulating a free surface (see Example Problem 1 in Ref [21, page 3-13]). Appendix A shows an example problem of a finite element modal analysis of a 5m closed-closed and closed-open tube.

An alternative method involves defining a Helmholtz resonator that has the same acoustic properties as the vent hole. The properties of this Helmholtz resonator would not be varied during the optimisation procedure.

4.4 Stage 4 Task 4. Incorporation of measured data into modeling and design tools

The FE modal data will be replaced with actual measured modal data for the structure, cavity and VADS to provide a more accurate prediction of the performance and determine the optimal configuration of VADS for best performance.

The success of this task is dependent on the cooperation from the group that supplies

the results from the experimental testing. The data that are required are the experimental modal analysis results of the structure and cavity. There are two alternate methods that can be used to make use of these data: finite element model update techniques, and interpolation and extrapolation of the data to obtain a full set of mode shapes and resonance frequencies. The finite element model update technique involves modification of the finite element model's mass and stiffness matrices until the mode shapes predicted using finite element methods match the experimentally measured results. The extrapolation and interpolation technique involves creating modal results at locations between the experimental measurement locations.

It is possible that this task is cannot be practically achieved in a reasonable amount of time. An alternative task that could replace this one involves examining the sensitivity of the acoustic loading condition to the change in the acoustic potential energy levels in the payload bay.

It is clear that an optimum solution for the location, mass, stiffness and damping of the PVADs is dependent on the acoustic loading conditions, as was seen in Stage 3A [4, page 29]. Researchers who are investigating the problem of reducing the noise inside the payload bay of launch vehicles all face the same problem of finding a suitable representation of the acoustic loading condition on the exterior of the fairing.

Estéve and Johnson [22] have assumed that an plane wave is incident on a cylinder from an elevated angle, by using the theory from Morse and Ingard [23, Ch 8-p400, Ch9-p511]. Gardonio et al. [13] assume a similar loading condition.

A picture of a typical launch pad configuration is shown in Figure 4.1. The exhaust from the rocket motor exits vertically downwards from the launch vehicle and is deflected to one or two sides. Sometimes there is a water injection system that is used to attenuate some of the rocket noise, as used on the shuttle launch system. The plume of exhaust could be modelled as a line source emanating from the launch pad. It likely that this noise source is more complex than a plane wave striking the cylinder at an angle.

However, given that the conditions for each launch are likely to be different, it would

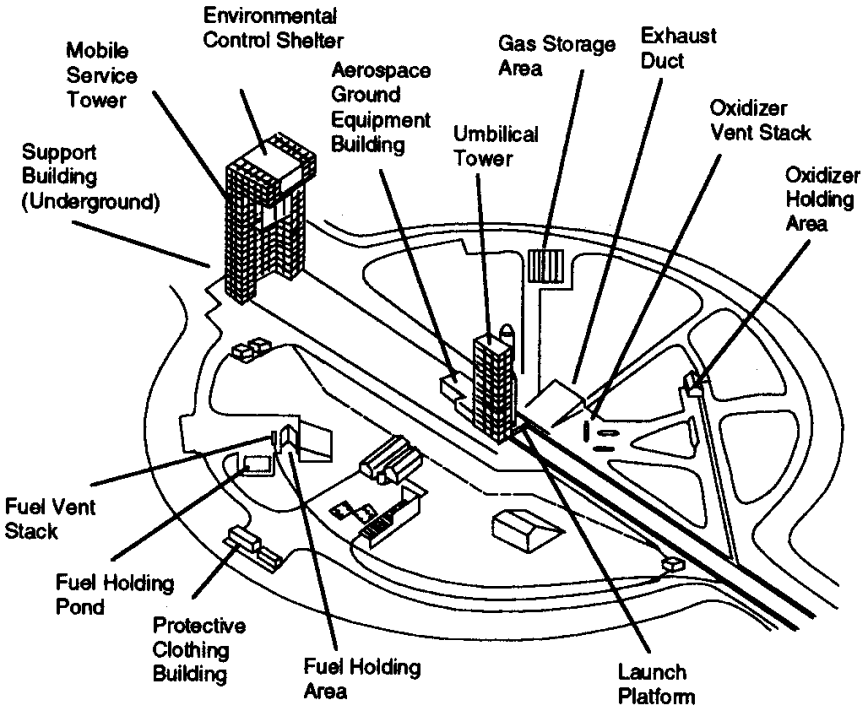

FIG. 4.1: Diagram of a typical launch pad configuration showing the exhaust chute.

be prudent to ensure that the noise control measures are relatively insensitive to the acoustic loading conditions. It is proposed that the acoustic potential energy levels inside the cylinder should be compared for several acoustic load cases:

- plane wave loading perpendicular to the axis of the rocket, as was done in Stage 3A.
- a series of point sources along a line below the payload fairing, to simulate noise sources from a two exhaust chutes.
- random phase over the exterior surface of the fairing.

An additional task is to compare actual noise reduction / transmission loss measurements of a payload fairing from acoustic tests conducted in a laboratory, with those predicted using the finite element models and modal coupling theory. This task can only be completed if the Airforce Research Laboratory can provide the experimental results with sufficient accuracy and at a sufficient number of test locations in the acoustic space. Results with and without PVADs installed would also be needed.

Chapter 5

Conclusions

5.1 Summary

In summary, the work that completed in this Stage 3B was

- Investigations were conducted on the use of mathematical techniques to reduce the calculation times of the coupled vibro-acoustic response. Methods that were investigated were the use of symmetric matrix formulations, pseudo-static correction factors. The results showed that there was benefit in re-coding the Matlab software to reduce the number of matrix multiplications, and the use of symmetric matrices reduces the calculation time. The use of pseudo-static correction factors is not likely to improve the accuracy without significant software development that is beyond the scope of this work.

- Comparisons were made between the use of integer and binary representations of the chromosomes for the genetic algorithm optimisation. It was found that the integer representation of the chromosomes achieved the same reduction in acoustical potential energy as the binary representation with half the number of cost function evaluations. Hence the integer representation shall be used for all future work.

- The feasibility of the four tasks planned for the Stage 4 work were investigated. The conclusion is that the first three tasks are all feasible, however the forth task,

Incorporation of Measured Data into Modeling and Design Tools, is very likely to cause logistical problems with obtaining sufficient and meaningful data from another party. It was suggested that an alternative task replace the task that is currently planned.

5.2 Future Work

The Stage 4 work will prosecute the plan described in this report.

Additional work will be done to reduce the calculation time of the coupled vibro-acoustic response, by attempting to implement a symmetric matrix formulation of the modal coupling theory, which incorporates the effects of the PVADs.

Appendix A

Modal Analysis of a Tube

The resonance frequencies of a closed-closed and closed-open tube were calculated using Ansys to demonstrate a technique that can be used to model a vent hole in the fairing. A free surface can be defined by applying a boundary condition of zero pressure. This follows from the example shown in Ref [21, page 3-13].

The theoretical resonance frequencies of a closed-closed tube are calculated as [11, p152] $f = nc/(2L)$ where $n = 0, 1, 2, \cdots$, c is the speed of sound in the fluid, L is the length of the tube. For a closed-open tube, the resonance frequencies are $f = nc/(4L)$ where $n = 1, 3, 5 \cdots$. For this example the length of the tube $L = 5$m and $c = 344$m/s. Figure A.1 shows the ANSYS model and Table A.1 lists the theoretical and ANSYS calculated resonance frequencies for the closed-closed and closed-open tube. The ANSYS calculated resonance frequencies are within about 1% of the theoretical values.

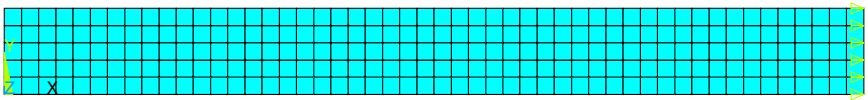

FIG. A.1: Ansys model of a closed-open tube.

Closed-Closed			Closed-Open		
Theory	ANSYS	% Diff	Theory	ANSYS	% Diff
0.0	0.0	0.0	17.2	17.2	0.0
34.4	34.4	0.0	51.6	51.6	0.0
68.8	68.8	0.1	86.0	86.1	0.1
103.2	103.4	0.1	120.4	120.6	0.2
137.6	138.0	0.3	154.8	155.3	0.3
172.0	172.7	0.4	189.2	190.1	0.5
206.4	207.6	0.6	223.6	225.2	0.7
240.8	242.8	0.8	258.0	260.4	0.9
275.2	278.1	1.1	292.4	295.9	1.2

Table A.1: Resonance frequencies of a closed-closed and closed-open tube.

Bibliography

[1] Carl Q. Howard'. *Active isolation of machinery vibration from flexible structures.* PhD thesis, Department of Mechanical Engineering, University of Adelaide, Adelaide, South Australia, Australia, 1999.

[2] Colin Hansen, Anthony Zander, Ben Cazzolato, and Rick Morgans. Investigation of passive control devices for potential application to a launch vehicle structure to reduce the interior noise levels during launch: Final report for stage 1. Technical report, Department of Mechanical Engineering, University of Adelaide, Adelaide, S.A. 5000, Australia, November 2000.

[3] Colin Hansen, Anthony Zander, Ben Cazzolato, and Rick Morgans. Investigation of passive control devices for potential application to a launch vehicle structure to reduce the interior noise levels during launch: Final report for stage 2. Technical report, Department of Mechanical Engineering, University of Adelaide, Adelaide, S.A. 5000, Australia, November 2000.

[4] Carl Olsard, Rick Morgans, Anthony Zander, and Colin Hansen. Investigation of passive control devices for potential application to a launch vehicle structure to reduce the interior noise levels during launch: Final report for stage 3a. Technical report, Department of Mechanical Engineering, University of Adelaide, Adelaide, S.A. 5005, Australia, September 2003.

[5] Ben S. Cazzolato. *Sensing systems for active control of sound transmissino into*

cavities. PhD thesis, Department of Mechanical Engineering, University of Adelaide, Adelaide, South Australia, Australia, 1999.

[6] Frank Fahy. *Sound and structural vibration: radiation, transmission and response*. Academic Press, San Diego, California, USA, 1985.

[7] V. B. Bokil and U. S. Shirahatti. A technique for the modal analysis of sound-structure interaction problems. *Journal of Sound and Vibration*, 173(1):23–41, 1994.

[8] Michel Tournour and Noureddine Atalla. Pseudostatic corrections for the forced vibroacoustic response of structure- cavity system. *Journal of the Acoustical Society of America*, 107(5):2379–2386, May 2000.

[9] Henri J.-P. Morand and Roger Ohayon. *Fluid structure interaction - applied numerical methods*. John Wiley and Sons, Paris, 1995. ISBN 0471944599.

[10] N. Atalla and R. J. Bernhard. Review of numerical soulutions for low-frequency structura-acoustic problems. *Applied Acoustics*, 43:271–294, 1994.

[11] Leo L. Beranek and Istvan L. Ver, editors. *Noise and vibration control engineering. Principles and applications.* John Wiley and Sons, U.S.A., 1992.

[12] Lorraine Olson and Thomas Vandini. Eigenproblems from finite element analysis of fluid-structure interactions. *Computers and Structures*, 33(3):679–687, 1989.

[13] P. Gardonio, N. S. Ferguson, and F. J. Fahy. A modal expansion analysis of noise transmission through circular cylindrical shell structures with blocking masses. *Journal of Sound and Vibration*, 244(2):259–297, 2001.

[14] Jonathan D. Kemp and Robert L. Clark. Noise reductin in a launch vehicle fairing using actively tuned loudspeakers. *Journal of the Acoustical Society of America*, 113 (4):1986–1994, April 2003.

[15] E. H. Dowell, G. F. Gorman III, and D. A. Smith. Acoustoelasticity: General theory, acoustic natural modes and forced response to sinusoidal excitation, including comparisons with experiment. *Journal of Sound and Vibration*, 52(4):519–542, 1977.

[16] You-qun Zhao, Su-huan Chen, San Chai, and Qing-wen Qu. An improved modal truncation method for responses to harmonic excitation. *Computers and Structures*, 80:99–103, 2002.

[17] Colin H. Hansen, Marc T. Simpson, and Ben S. Cazzolato. *Active sound and vibration control: theory and applications*, chapter 9: Genetic algorithms for optimising ASVC systems, pages 185–220. Number 62 in IEE control engineering series. Institution of Electrical Engineers, London, UK, 2002.

[18] Marc T. Simpson and Colin H. Hansen. Use of genetic algorithms for optimizing vibration actuator placement for minimizing sound transmission into enclosed spaces. In *Proceedings of SPIE - The International Society for Optical Engineering, Smart Structures and Materials 1996: Smart Structures and Integrated Systems*, 1996.

[19] Colin H. Hansen, Marc T. Simpson, and Ben S. Cazzolato. Genetic algorithms for active sound and vibration control. In *Inter-Active 99*, 1999.

[20] Carl Q. Howard, Colin H. Hansen, and J. Q. Pan. Power transmission from a vibrating body to a circular cylindrical shell through active elastic isolators. *Journal of the Acoustical Society of America*, 101(3):1479–1491, 1997.

[21] David B. Woyak. *Ansys: Acoustics and Fluid Structure Interaction: a revision 5.0 tutorial*. Swanson Analysis Systems Inc., Houston, PA, USA, June 1992.

[22] Simon J Estéve and Marty E Johnson. Reduction of sound transmission into a circular cylinderical shell using distributed vibration absorbers and helmholtz resonators. *Journal of the Acoustical Society of America*, 112(6):2840–2848, December 2002.

[23] M. Morse and K. U. Ingard. *Theoretical Acoustics*. McGraw-Hill, New York, USA, 1986.

[24] Jianmin Gu, Zheng-Dong Ma, and Gregory M. Hulbert. Quasi-static data recovery for dynamic analyses of structural systems. *Finite Elements in Analysis and Design*, 37:825–841, 2001.